CLASSIFICATION OF TOTALLY REAL ELLIPTIC LEFSCHETZ FIBRATIONS VIA NECKLACE DIAGRAMS

NERMİN SALEPCİ

Abstract. We show that totally real elliptic Lefschetz fibrations admitting a real section are classified by their "real loci" which can be encoded in terms of a combinatorial object that we call a *necklace diagram*. By means of necklace diagrams, we obtain an explicit list of certain classes of totally real elliptic Lefschetz fibrations.

1. Introduction

As is well known, a Lefschetz fibration is a projection from an oriented connected smooth 4-manifold onto an oriented connected smooth surface such that there exist finitely many critical points around which one can choose complex charts on which the projection takes the form $(z_1, z_2) \to z_1^2 + z_2^2$. Regular fibers of a Lefschetz fibration are oriented closed smooth surfaces of genus g, while singular fibers have only nodes. In the present work, we consider only those fibrations whose fiber genus is 1. We call such fibrations *elliptic Lefschetz fibrations*. Without loss of generality, we assume that each singular fiber contains only one node and that no fiber contains a self intersection -1 sphere (fibrations with the latter property are called *relatively minimal*).

We study *real elliptic Lefschetz fibrations*; that is to say, elliptic Lefschetz fibrations whose total and base spaces have *real structures* which are compatible with the fiber structure. A *real structure* on an oriented smooth 4-manifold is defined as an orientation preserving involution whose fixed point set (called the *real part*) has dimension 2, if it is not empty. Two real structures are considered the same if they differ by a conjugation by an orientation preserving diffeomorphism. It is worth mentioning here that not every 4-manifold admits such an involution. Examples of 4-manifolds which do not admit real structures can be found in [3]. Likewise, a *real structure* on a smooth oriented surface is defined as an orientation reversing involution. Obviously every surface admits a real structure. Besides, the classification (up to conjugation by an orientation preserving diffeomorphism) of real structures on surfaces is known. There are two invariants that determine the conjugacy class of a real structure: its type (separating/non-separating) and the number of the components of its real part. A real structure is called *separating* if the real part divides the surface into two disjoint halves; otherwise, it is called *non-separating*. Throughout the present work, we focus on fibrations over S^2, and the real structure considered on S^2 is the one induced from the complex conjugation, denoted *conj*, on $\mathbb{C}\mathrm{P}^1$. By definition of real Lefschetz fibrations, fibers over the real part S^1 of

The author was partially supported by the European Community's Seventh Framework Programme ([FP7/2007-2013] [FP7/2007-2011]) under grant agreement no[258204], as well as by the French *Agence nationale de la recherche* grant ANR-08-BLAN-0291-02.

conj inherit real structures from the real structure of the total space. Such fibers are called *real (fibers)*. A real elliptic Lefschetz fibration has 3 types of real regular fibers. They are distinguished by the number of real components that can be $0, 1, 2$ (only the structure with 2 real components is separating on T^2).

For the sake of simplicity, most of the time we assume that the real part S^1 of $(S^2, conj)$ is oriented. Fibrations with such a feature are called *directed*. Moreover, we consider mainly fibrations which admit a *real section* (a section compatible with the real structures). But the cases of non-directed fibrations as well as of fibrations without a real section are also covered. The only essential condition imposed on fibrations is that all the critical values are real. Fibrations with this property are called *totally real*.

Our main interest is the topological classification of totally real elliptic Lefschetz fibrations. Two real Lefschetz fibrations will be considered *isomorphic* if they differ by orientation preserving equivariant diffeomorphisms. Recall that the classification of elliptic Lefschetz fibrations over S^2 has been known for over 30 years. It is due to B. Moishezon and R. Livné [4] that (non-real, relatively minimal) elliptic Lefschetz fibrations over S^2 are classified (up to isomorphism) by the number of the critical values. The latter is divisible by 12 and the class of elliptic Lefschetz fibrations with $12n$ critical values is denoted by $\mathrm{E}(n)$, $n \in \mathbb{N}$. Furthermore, $\mathrm{E}(1)$ is isomorphic to the fibration $\mathbb{C}\mathrm{P}^2\#9\overline{\mathbb{C}\mathrm{P}^2} \to \mathbb{C}\mathrm{P}^1$, obtained by blowing up a pencil of cubics in $\mathbb{C}\mathrm{P}^2$, and $\mathrm{E}(n) = \mathrm{E}(n-1)\sharp_F\mathrm{E}(1)$ where $\sharp_F$ stands for the fiber sum.

In this note, we give the real version of this result for totally real elliptic Lefschetz fibrations. The classification is obtained by means of certain combinatorial objects that we call *necklace diagrams*. Necklace diagrams are combinatorial counterparts of *real Lefschetz chains* introduced in [6].

Main results of this work are presented as Theorem 4.1 and Theorem 7.1 in which we treat the cases of directed totally real elliptic Lefschetz fibrations admitting a real section and, respectively, those fibrations possibly without a real section. As immediate corollaries (Corollary 4.4, respectively, Corollary 7.2) of these theorems, we obtain that non-directed totally real elliptic Lefschetz fibrations admitting a section are classified by their necklace diagrams (defined up to symmetry and with the identity monodromy), while those fibrations possibly without a real section are classified by the symmetry classes of their *refined* necklace diagrams with the identity monodromy. As a consequence of Corollary 4.4, we obtain an explicit list of totally real $\mathrm{E}(1)$ and $E(2)$ that admit a real section. We investigate the algebraic realizations of these fibrations and show that certain fibrations on the list are not algebraically realizable. We also consider some operations on the set of necklace diagrams: *mild/harsh sums*, *flip-flops* and *metamorphoses*. These operations allow us to construct new necklace diagrams from the given ones. By means of these operations, we construct an example of a real Lefschetz fibration which cannot be written as a fiber sum of two real fibrations (see Proposition 6.5).

Acknowledgements. The material presented here is extracted from my thesis. I am deeply indebted to my supervisors Sergey Finashin and Viatcheslav Kharlamov for their guidance and limitless support. I owe many thanks to Andy Wand who wrote the program to get the explicit list of necklace diagrams, who also edited my present and past articles as a native english speaker. I thank Alex Degtyarev for his precious comments on the first manuscript and for productive discussions.

The article has been finalized during my visit to the Mathematisches Forschungsinstitut Oberwolfach as an "Oberwolfach Leibniz fellow". I would like to thank the institute for providing me exquisite working conditions.

2. Real loci of real elliptic Lefschetz fibrations and necklace diagrams

Let $\pi : X \to \mathrm{S}^2$ be a directed real elliptic Lefschetz fibration. Consider the restriction, $\pi_{\mathbb{R}} : X_{\mathbb{R}} \to \mathrm{S}^1$, of π to the real part $X_{\mathbb{R}}$ of X. By definition, fibers of $\pi_{\mathbb{R}}$ are the real parts of the real fibers of π. The base S^1 is oriented (as $\pi : X \to S^2$ is directed), whereas the total space $X_{\mathbb{R}}$ is either empty or a surface not necessarily oriented nor connected.

By definition of real Lefschetz fibrations, the map $\pi_{\mathbb{R}}$ is an S^1-valued Morse function on $X_{\mathbb{R}}$ whose regular fibers can be S^1, $\mathrm{S}^1 \amalg \mathrm{S}^1$ or the empty set. On the other hand, singular fibers are either a wedge of two circles (this occurs in the case when the critical point is of index 1) or a disjoint union of S^1 with an isolated point or just an isolated point (these cases occur when the critical point is of index 0 or 2). As an immediate consequence, we note that the real part $X_{\mathbb{R}}$ is not empty if π has a real critical value. (We consider fibrations with real critical values, so $X_{\mathbb{R}}$ will never be empty throughout this article.)

For the sake of simplicity, we first focus on fibrations which admit a real section. By a real section, we understand a section $s : \mathrm{S}^2 \to X$ commuting with the real structures. Existence of a real section assures that fibers of $\pi_{\mathbb{R}}$ are never empty, so there are only two possible topological types for regular fibers: S^1 or $\mathrm{S}^1 \amalg \mathrm{S}^1$.

We now introduce a decoration on the base S^1 of $\pi_{\mathbb{R}} : X_{\mathbb{R}} \to \mathrm{S}^1$ as follows. First, label the critical values of $\pi_{\mathbb{R}}$ by "$\times$" or "$\circ$" according to the parity of indices of the corresponding critical points. Namely, if the corresponding critical point is of index 1, label the critical value by "$\times$", otherwise by "$\circ$". (Note that $\pi_{\mathbb{R}}$ has critical values as long as π has real critical values.) Second, consider a labeling on the set of *regular intervals*, $\mathrm{S}^1 \setminus \{\text{critical values}\}$. Over each regular interval the topology of the fibers of $\pi_{\mathbb{R}}$ is fixed; moreover, it alternates as we pass through a critical value. We label regular intervals over which fibers have two components by doubling the interval, see Figure 1. Intervals over which the fibers are a copy of S^1 remain unlabeled. The oriented base S^1 together with such a decoration is called an *oriented uncoated necklace diagram*.

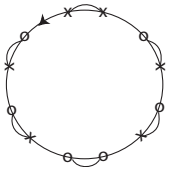

Fig. 1. An example of an uncoated necklace diagram.

We consider some "standard" pieces out of which all possible uncoated necklace diagrams can be built. It is convenient for us to take pieces with two consecutive critical values (in order to avoid the problem of matching real structures). Let us choose a regular value on S^1 (for some later use we choose the point on an unlabeled regular interval). With respect to this point and the orientation of S^1, we have 4

instances for a pair of two critical values. In order to simplify the decoration, for each instance we introduce a new notation as shown in Figure 2.

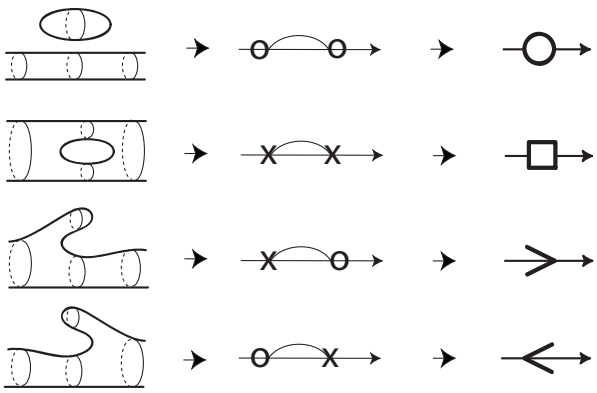

FIG. 2. Portions of the $X_{\mathbb{R}}$ and the pieces of uncoated necklace diagrams, and corresponding necklace stones.

The oriented S^1 decorated using elements of the set $S = \{\bigcirc, \square, >, <\}$ is called an *oriented necklace diagram* (an example is shown in Figure 3). We call the elements of the set S *(necklace) stones* and the pieces of the circle between the stones *(necklace) chains*. Two oriented necklace diagrams are considered identical if they contain the same types of stones going in the same cyclic order.

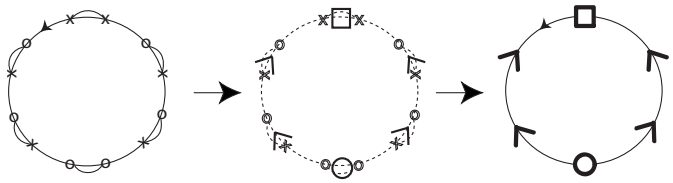

FIG. 3. A necklace diagram.

It is obvious from the construction that oriented necklace diagrams are invariants of directed real elliptic Lefschetz fibrations. For non-directed real Lefschetz fibrations, we do not have a preferable orientation on the necklace diagram. Non-directed fibrations, hence, determine a pair of oriented necklace diagrams related by a mirror symmetry in which $\bigcirc$-type and $\square$-type stones remain unchanged, while $>$-type and $<$-type stones interchanged.

3. Monodromy representations of stones

Monodromies of real Lefschetz fibrations along certain loops (namely, loops on which the real structure acts as a reflection) can be written as a composition of two real structures, see [5]. In particular, the monodromy around a real singular fiber can be written as $t_a = c' \circ c$ where t_a denotes the positive Dehn twist along the vanishing cycle a on a (non-real) marked fiber $F \cong T^2$ and c, c' are the real structures pulled back from the nearby real fibers. (If the fibration is directed, we

choose the marked fiber so that c and c' are the real structures acquired from the left and, respectively, right real fibers).

Recall that monodromy of elliptic Lefschetz fibrations are elements of the mapping class group $Map(\mathrm{T}^2)$ (the group of isotopy classes of orientation preserving diffeomorphisms) of the torus. It is known that $Map(\mathrm{T}^2)$ is isomorphic to the group of orientation preserving automorphisms of $H_1(T^2,\mathbb{Z}) \cong \mathbb{Z}u \oplus \mathbb{Z}v$. The latter is known to be isomorphic to $\mathrm{SL}(2,\mathbb{Z})$.

Let $\mathrm{T}^2 \cong \mathrm{S}^1 \times \mathrm{S}^1$ so that $u = \mathrm{S}^1 \times \{0\}$ and $v = \{0\} \times \mathrm{S}^1$. Then, we consider two presentations of $Map(\mathrm{T}^2) \simeq \mathrm{SL}(2,\mathbb{Z})$:

$$\begin{aligned}\mathrm{SL}(2,\mathbb{Z}) &= \left\{ [t_u] = \begin{pmatrix} 1 & 1 \\ 0 & 1 \end{pmatrix} \text{ and } [t_v] = \begin{pmatrix} 1 & 0 \\ -1 & 1 \end{pmatrix} : \begin{array}{l} [t_u][t_v][t_u] = [t_v][t_u][t_v] \\ ([t_u][t_v])^6 = \mathrm{id} \end{array} \right\} \\ &= \{x = \begin{pmatrix} 0 & 1 \\ -1 & 0 \end{pmatrix} \text{ and } y = \begin{pmatrix} 0 & 1 \\ -1 & 1 \end{pmatrix} : x^2 = y^3, x^4 = \mathrm{id}\}\end{aligned}$$

where t_w denotes the Dehn twists along w and $[t_w]$ is the matrix representation of the induced isomorphism t_w*. One can switch from the first presentation to the second by setting $x = [t_u][t_v][t_u] = [t_v][t_u][t_v]$ and $y = [t_u][t_v]$.

Each real structure, $c : \mathrm{T}^2 \to \mathrm{T}^2$, induces an isomorphism c_* on $H_1(\mathrm{T}^2,\mathbb{Z}) \cong \mathbb{Z}u \oplus \mathbb{Z}v$ that defines two rank 1 subgroups $H^c_\pm(T^2) = \{\gamma \in H_1(\mathrm{T}^2,\mathbb{Z}) : c_*\gamma = \pm\gamma\}$. (If c has one real component, then $H_1(\mathrm{T}^2,\mathbb{Z})/ < H^c_+, H^c_- >= \mathbb{Z}/2\mathbb{Z}$, otherwise, $H_1(\mathrm{T}^2,\mathbb{Z}) = H^c_+ \oplus H^c_-$.) Moreover, a real structure c on a real fiber F defines a pair of bases $\pm(u,v)$ so that $u \pm v$ generates $H^c_\pm$. This defines a canonical identification of $H_1(F,\mathbb{Z})$ to $H_1(T^2,\mathbb{Z})$.

To each decoration around a critical value q, we assign the transition matrix P_q from a basis of $H^c_+ \oplus H^c_- \subset H_1(T^2,\mathbb{Z})$ to a basis of $H^{c'}_+ \oplus H^{c'}_- \subset H_1(T^2,\mathbb{Z})$ where c, c' are left and, respectively, right real structures on the real fibers near F_q.

Lemma 3.1. *For each decoration around a critical value, we get the following matrices defined up to sign.*

$$\begin{aligned} \mathrm{P}_{-\times<} &= \tfrac{1}{2}\begin{pmatrix} 1 & 0 \\ -1 & 2 \end{pmatrix}, & \mathrm{P}_{>\times-} &= \begin{pmatrix} 2 & 0 \\ -1 & 1 \end{pmatrix}, \\ \mathrm{P}_{-\circ<} &= \tfrac{1}{2}\begin{pmatrix} 2 & 1 \\ 0 & 1 \end{pmatrix}, & \mathrm{P}_{>\circ-} &= \begin{pmatrix} 1 & 1 \\ 0 & 2 \end{pmatrix}. \end{aligned}$$

Remark 3.2. By definition of real Lefschetz fibrations, around each critical point and its image, one can choose equivariant local (closed) charts on which the fibration is equivariantly isomorphic to either of $\xi_\pm : (E_\pm, conj) \to (D_\epsilon, conj)$, where $E_\pm = \{(z_1,z_2) \in \mathbb{C}^2 : |z_1| \le \sqrt{\epsilon}, \left|z_1^2 \pm z_2^2\right| \le \epsilon^2\}$ and $D_\epsilon = \{t \in \mathbb{C} : |t| \le \epsilon^2\}$, $0 < \epsilon < 1$ with $\xi_\pm(z_1,z_2) = z_1^2 \pm z_2^2$. From the models $\xi_\pm$ one can see immediately that in the case of ξ_+ (this is the model for the critical point of index 0, 2) there are two types of real regular fibers distinguished by their real parts. In both types, one can choose an invariant representative of the vanishing cycle, and the action of the real structure on the invariant representative can be either the antipodal map or the identity. On the other hand, in the case of ξ_- (this is the case of critical points of index 1) the real structure acts on the invariant representative of the vanishing cycle as a reflection. Consequently, in the former situation (which corresponds to the decoration "$\circ$") the class of the vanishing cycle gives an element in H^c_+,

while in the latter case (the case corresponding to the decoration "$\times$") the class of the vanishing cycle gives an element of H^c_-. (A detailed discussion about the local models can be found in [6, Section 3] where the above claims are depicted in Figure 2.)

Proof: Explicit calculations are made for $\mathrm{P}_{-\times<}$ and $\mathrm{P}_{>\circ-}$; the other cases are similar.

Let q be a critical value. We consider a sufficiently small ϵ-neighborhood $D_q \subset \mathrm{S}^2$ of q such that $conj(D_q) = D_q$ and $D_q \cap \{\text{critical values}\} = q$ and choose a non-real point m on ∂D_q. By means of the shortest paths on ∂D_q from m to the left $q-\epsilon$ and right $q+\epsilon$ real points of ∂D_q, we pull the real structures on $F_{q\pm\epsilon}$ back to F_m. Fix an auxiliary identification T^2 with the fiber F_m and let $c : \mathrm{T}^2 \to \mathrm{T}^2$ (respectively, $c' : \mathrm{T}^2 \to \mathrm{T}^2$) be the real structure obtained by pulling back the real structure on $F_{q-\epsilon}$ (respectively, $F_{q+\epsilon}$) so that the (local) monodromy is the composition $c' \circ c$.

The case of $(-\times <)$: as discussed in Remark 3.2, the critical value of the type "$\times$" provides a generator of $H^c_- \subset H_1(\mathrm{T}^2, \mathbb{Z})$. Let b denote the corresponding vanishing cycle and β the homology class of b. Set $< \beta >= H^c_-$ and choose a generator α for H^c_+ such that $\alpha \cdot \beta = 2$ (since c has one real component). From the local monodromy decomposition, we get $c'_* = t_{b*} \circ c_*$; therefore,

$$\begin{array}{rcl} c'_*(\alpha) & = & t_{b*}(c_*(\alpha)) = \alpha - 2\beta \\ c'_*(\beta) & = & t_{b*}(c_*(\beta)) = -\beta. \end{array}$$

Obviously, the class $\alpha + c'_*(\alpha) = 2\alpha - 2\beta \in H^{c'}_+$, while $\beta - c'_*(\beta) \in H^{c'}_-$. We set $\alpha' = \frac{\alpha-\beta}{2}$ and $\beta' = \beta$ so that we have $B' = (\alpha', \beta')$ with $< \alpha' >= H^{c'}_+$ and $< \beta' >= H^{c'}_-$. Then, $\mathrm{P}_{-\times<} = \frac{1}{2}\begin{pmatrix} 1 & 0 \\ -1 & 2 \end{pmatrix}$.

The case of $(> \circ -)$: we repeat the same with the difference that the vanishing cycle a gives a generator α for H^c_+, and we choose a generator β for H^c_- so that $\alpha \cdot \beta = 1$ (the left real structure c is separating). From the local monodromy decomposition, we get

$$\begin{array}{rcl} c'_*(\alpha) & = & \alpha \\ c'_*(\beta) & = & t_{a*}(c_*(\beta)) = -\beta - \alpha. \end{array}$$

Therefore, $\alpha' = \alpha$ and $\beta' = \beta - c'_*(\beta) = 2\beta + \alpha$ is a basis of $H^{c'}_+$ and, respectively, of $H^{c'}_-$; thus, $\mathrm{P}_{>\circ-} = \begin{pmatrix} 1 & 1 \\ 0 & 2 \end{pmatrix}$.

(As $\alpha \cdot \beta > 0$ if and only if $(-\alpha)\cdot(-\beta) > 0$, the matrices are defined up to sign.) $\square$

Remark 3.3. Intuitively, the monodromy assigned to a decoration around a critical value can be interpreted as the *half* of the monodromy around the real critical value. Namely, it is the monodromy assigned to the path shown in Figure 4. It is straightforward to check that $\mathrm{P}_{-\times<} = M P^{-1}_{>\times-} M$ and $\mathrm{P}_{-\circ<} = M P^{-1}_{>\circ-} M$ where $M = M^{-1} = \begin{pmatrix} 1 & 0 \\ 0 & -1 \end{pmatrix}$. Moreover, one observes that

$$\mathrm{P}_{>\times-}\mathrm{P}_{-\times<} = (\mathrm{P}_{>\times-})(M\mathrm{P}^{-1}_{>\times-}M) = [t_v]_B$$

where $[t_v]_B$ denotes the matrix of t_{v*} with respect to the base $B = (\alpha, \beta)$. Similarly, one has $\mathrm{P}_{>\circ-}\mathrm{P}_{-\circ<} = [t_u]_B$ as well as $\mathrm{P}_{-\times<}\mathrm{P}_{>\times-} = [t_v]_{B'}$ and $\mathrm{P}_{-\circ<}\mathrm{P}_{>\circ-} = [t_u]_{B'}$ where $B' = (\alpha', \beta')$.

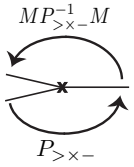

FIG. 4. An example of a decomposition of the monodromy associated to the decoration of a real critical value.

Following Lemma 3.1, to each necklace stone, we assign the following products (defined up to sign).

$$\begin{aligned}
\mathrm{P}_{\square} &= \mathrm{P}_{-\times<}\mathrm{P}_{>\times-} &&= \begin{pmatrix} 1 & 0 \\ -2 & 1 \end{pmatrix},\\
\mathrm{P}_{\bigcirc} &= \mathrm{P}_{-\circ<}\mathrm{P}_{>\circ-} &&= \begin{pmatrix} 1 & 2 \\ 0 & 1 \end{pmatrix},\\
\mathrm{P}_{>} &= \mathrm{P}_{-\times<}\mathrm{P}_{>\circ-} &&= \tfrac{1}{2}\begin{pmatrix} 1 & 1 \\ -1 & 3 \end{pmatrix},\\
\mathrm{P}_{<} &= \mathrm{P}_{-\circ<}\mathrm{P}_{>\times-} &&= \tfrac{1}{2}\begin{pmatrix} 3 & 1 \\ -1 & 1 \end{pmatrix}.
\end{aligned}$$

Because we choose the marked point on an unlabeled interval, the matrices have coefficients in $\frac{1}{2}\mathbb{Z}$. If the marked point was chosen on a labeled interval, the matrices would be elements of $\mathrm{PSL}(2,\mathbb{Z})$. (The reason why we prefer a point on an unlabeled interval is to get a nice relation between necklace stones and the real part, see Remark 4.6.) The subgroup generated by $\{\mathrm{P}_{\bigcirc}, \mathrm{P}_{\square}, \mathrm{P}_{>}, \mathrm{P}_{<}\}$ is conjugate to $\mathrm{PSL}(2,\mathbb{Z}) = \{x, y : x^2 = y^3 = \mathrm{id}\}$. To be able to work with $\mathrm{PSL}(2,\mathbb{Z})$, we consider the following lemma.

Lemma 3.4. *Let* $\mathrm{R} = \frac{1}{2}\begin{pmatrix} 1 & -1 \\ 1 & 1 \end{pmatrix}$ *and* $\mathbb{P} = \mathrm{R}^{-1}\mathrm{PR}$.

Then, for each necklace stone, we obtain the following factorization.

$$\begin{aligned}
\mathbb{P}_{\square} &= yxy\\
\mathbb{P}_{\bigcirc} &= xyxyx\\
\mathbb{P}_{>} &= y^2x\\
\mathbb{P}_{<} &= xy^2
\end{aligned}$$

Proof: It follows from the observation that $\mathbb{P}_{>} = [t_u]$, $\mathbb{P}_{<} = [t_v]$, while $\mathbb{P}_{\square} = [t_u][t_v][t_u]^{-1}$, $\mathbb{P}_{\bigcirc} = [t_u]^{-1}[t_v][t_u]$. □

The matrices $\mathbb{P}_{\bigcirc}, \mathbb{P}_{\square}, \mathbb{P}_{>}, \mathbb{P}_{<}$ are called *monodromies of stones*. The product (with respect to a chosen marked point and to the orientation) of monodromies of necklace stones is called the *monodromy relative to the marked point* of the oriented necklace diagram. The *monodromy* of an oriented necklace diagram is, thus, defined as the conjugacy class of its monodromy relative to a marked point.

Proposition 3.5. *Let* $\pi : X \to \mathrm{S}^2$ *be a directed totally real elliptic Lefschetz fibration admitting a real section. Then, the monodromy of the oriented necklace diagram associated with* π *is the identity in* $\mathrm{PSL}(2,\mathbb{Z})$.

Proof: Let $\{s_1, \dots, s_k\}$ be the ordered set of stones of an oriented necklace diagram (order is given with respect to the orientation and a marked point) and $\mathbb{P} = \mathbb{P}_1\mathbb{P}_2 \dots \mathbb{P}_k$ be the monodromy of the necklace diagram relative to the marked point where each $\mathbb{P}_i$ is the monodromy of the stone s_i. By reinterpreting Remark 3.3 in terms of the matrices $\mathbb{P} = \mathrm{R}^{-1}\mathrm{PR}$ associated to necklace stones, the monodromy along a curve surrounding all real critical values can be written as the product $\mathbb{P}_1\mathbb{P}_2 \dots \mathbb{P}_k T \mathbb{P}_k^{-1} \dots \mathbb{P}_2^{-1}\mathbb{P}_1^{-1}T$, where $T = T^{-1} = \mathrm{R}^{-1}M\mathrm{R} = \left(\begin{smallmatrix} 0 & 1 \\ 1 & 0 \end{smallmatrix}\right)$ (see Figure 5).

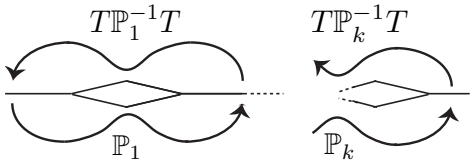

FIG. 5. A decomposition of the total monodromy.

If there is no non-real critical value, the monodromy along the curve we consider is identical to the total monodromy of the fibration which is the identity. Thus, $\mathbb{P}\left(\begin{smallmatrix} 0 & 1 \\ 1 & 0 \end{smallmatrix}\right)\mathbb{P}^{-1}\left(\begin{smallmatrix} 0 & 1 \\ 1 & 0 \end{smallmatrix}\right) = \mathrm{id}$ (since everything conjugate to the identity is the identity). The equality assures that $\mathbb{P}$ is a diagonal matrix, hence it is the identity in $\mathrm{PSL}(2, \mathbb{Z})$. □

Remark 3.6. An important observation is that $\mathbb{P}_{\bigcirc} = x\mathbb{P}_{\square}x$ and $\mathbb{P}_{<} = x\mathbb{P}_{>}x$. Hence, if a necklace diagram has the identity monodromy, then the necklace diagram obtained from the original by replacing each □-type stone with ○-type stone, and each $>$-type stone with $<$-type stone and vice versa, has also the identity monodromy. Necklace diagrams obtained in this manner are called *dual necklace diagrams*.

Remark 3.7. Although for the moment, we focus on fibrations admitting a real section (hence, we consider only the case of real fibers with non-empty real part), it is worth mentioning the case of real fibers with empty real part. It is well known that the real structures with no real component and with two real components are isotopic to each other as orientation reversing diffeomorphisms, although they are two non-isotopic real structures. As a result, they induce the same isomorphism on the homology group; hence, monodromy calculations remain the same if the real structure with two real components is replaced by a real structure with no real component.

4. The correspondence theorems and consequences

Theorem 4.1. *There exists a one-to-one correspondence between the set of oriented necklace diagrams with* $6n$ *stones and with the identity monodromy and the set of isomorphism classes of directed totally real elliptic Lefschetz fibrations* $\mathrm{E}(n)$*,* $n \in \mathbb{N}$*, that admit a real section.*

Proof: The discussions in the previous sections and Proposition 3.5 result in an injection from the set of classes of directed totally real elliptic Lefschetz fibrations admitting a real section to the set of oriented necklace diagrams with identity monodromy. We want to show that this injection is also well-defined and surjective. To this end, first recall that the decoration on critical values determines the isotopy class of the vanishing cycle. (Thus, it determines the (non-real) isomorphism class of a small neighborhood of the singular fiber.) Whereas, the decoration on regular intervals determines the type of the real structure on the fibers over the intervals. The decoration around a critical value, hence, dictates a conjugacy class of the pair (c, a) where c is the real structure on the chosen nearby real fiber and a is the vanishing cycle such that $c(a) = a$. In [6], we call such a pair a *real code* and show that the isomorphism class of an equivariant neighborhood of a real singular fiber is determined by the conjugacy class of a real code (see [6, Section 3]). An oriented necklace diagram, therefore, defines an ordered sequence of the conjugacy classes of real codes up to cyclic order. Such a sequence is called a *real Lefschetz chain* in [6], the result, thus, follows from [6, Proposition 8.5]. □

Remark 4.2. It is easy to be convinced that the real code (c, a) determines the isomorphism type of an equivariant neighborhood of a singular fiber. In the case of elliptic fibrations admitting a real section, it is also easy to see that ordered sequence of real codes considered up to cyclic order is enough to recover the isomorphism type of the corresponding totally real fibration. This is because the totally real fibrations can be constructed by successive *fiber sums* (connected sums preserving the fiber structure) of equivariant neighborhoods. The crucial point is that the fiber sum operation is well-defined due to the contractibility of the components of the space diffeomorphisms the torus with a marked point. (A detailed discussion can be found in [6] where we cover the cases of higher genus fibrations as well as genus 1 fibrations without a section.)

Remark 4.3. As mentioned in [6, Remark 3.6], in the case when the regular fibers are tori, there are 6 conjugacy classes of real codes. Whereas, around each critical value we have 4 different decorations $\{-\times <, > \times -, -\circ <, > \circ -\}$. These decorations are exactly 4 of the 6 possible real codes on T^2. The other two cases appear in the case of non-existence of a real section that we discuss in the last section.

Corollary 4.4. *There exists a bijection between the set of symmetry classes of non-oriented necklace diagrams with* $6n$ *stones and with the identity monodromy and the set of isomorphism classes of non-directed totally real* $\mathrm{E}(n)$*,* $n \in \mathbb{N}$ *which admit a real section.* □

Each necklace diagram defines a decomposition of the identity in $\mathrm{PSL}(2, \mathbb{Z})$ into a product of $6n$ elements that are chosen from the set of monodromies of necklace stones. There is a simple algorithm to find all necklace diagrams associated with $\mathrm{E}(n)$. Applying the algorithm, we obtain the complete list of necklace diagrams of $\mathrm{E}(1)$. Later Andy Wand wrote a computer program which works for $n = 1, 2$.

The following theorem concerns $n = 1$.

Theorem 4.5. *There exist precisely 25 isomorphism classes of non-directed totally real* $\mathrm{E}(1)$ *admitting a real section. These classes are characterized by the non-oriented necklace diagrams presented in Figure 6.*

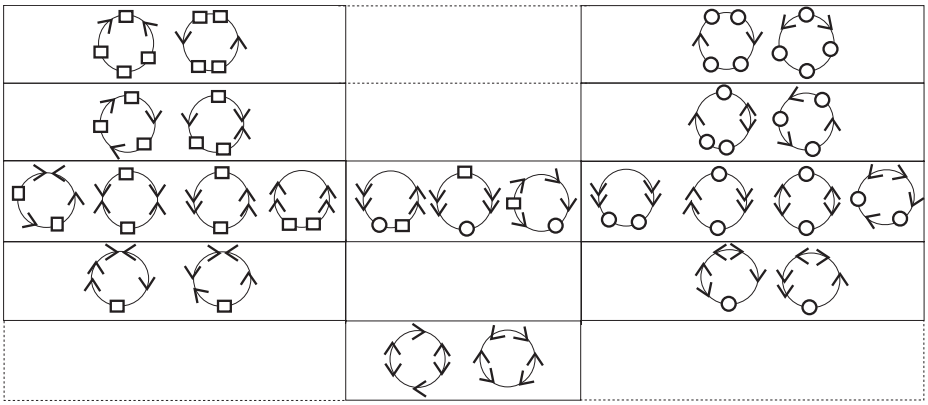

FIG. 6. List of necklace diagrams of totally real E(1) admitting a real section.

Proof: By Corollary 4.4, it is enough to find the list of symmetry classes of 6- stone necklace diagrams whose monodromy is the identity. Each necklace diagram defines a decomposition of the identity in $\mathrm{PSL}(2,\mathbb{Z}) = \{x, y : x^2 = y^3 = \mathrm{id}\}$ into a product of elements yxy, $xyxyx$, xy^2, y^2x. Let $S = yxy, C = xyxyx, L = xy^2, R = y^2x$. Then,

- first consider all the words of length 6 of letters S, C, L, R such that the product is the identity;
- then, (to get list of all oriented necklace diagrams which have the identity monodromy) quotient out the words which are equivalent to each other up to cyclic ordering;
- finally, quotient out the symmetry classes: in terms of words composed of the letters S, C, L, R, symmetry classes can be interpreted as follows: two words are considered to be equivalent if up to cyclic ordering, one is the reversed of the other with each L is replaced by R, and vice versa. For example, $CLLSRR \sim LLSRRC$.

□

It is worth mentioning here that there are 8421 necklace diagrams of 12 stones with the identity monodromy. Below, in Proposition 4.9, we give an explicit list of necklace diagrams corresponding to certain classes. Later, we also explore some interesting examples.

Remark 4.6. The topological invariants of $X_{\mathbb{R}}$ can be read from the necklace diagram of $\pi : X \to \mathrm{S}^2$. Namely, $\beta_0(X_{\mathbb{R}}) = \beta_2(X_{\mathbb{R}}) = |\bigcirc| + 1$ and $\beta_1(X_{\mathbb{R}}) = 2(|\square| + 1)$ where β_i denotes the i^{th} Betti number (with $\mathbb{Z}_2$ coefficients) and $|\bigcirc|$, $|\square|$ denote the number of $\bigcirc$-type and, respectively, $\square$-type stones of the necklace diagram associated with $\pi_{\mathbb{R}}$. Consequently, we have the Euler characteristic $\chi(X_{\mathbb{R}}) = 2(|\bigcirc| - |\square|)$, and the total Betti number $\beta_*(X_{\mathbb{R}}) = 2(|\bigcirc| + |\square|) + 4$.

Recall that in general we have $\beta_*(X_{\mathbb{R}}) \leq \beta_*(X)$ (known as *Smith inequality*). It is known that $\beta_*(\mathrm{E}(n)) = 12n$ ([2]), so the Smith inequality implies that $\beta_*(\mathrm{E}(n)_{\mathbb{R}}) \leq 12n$.

Proposition 4.7. *Each $6n$-stone necklace diagram with the identity monodromy contains at least two arrow-type stones.*

Proof: As mentioned above $\beta_*(\mathrm{E}(n)_{\mathbb{R}}) \leq 12n$. Meanwhile, we have $\beta_*(\mathrm{E}(n)_{\mathbb{R}}) = 2(|\bigcirc| + |\square|) + 4$. Thus, $|\bigcirc| + |\square| \leq 6n - 2$ on a $6n$-stone necklace diagram, so there are at least two arrow-type stones. □

Definition 4.8. A real structure c_X on X is called *maximal* if $\beta_*(X_{\mathbb{R}}) = \beta_*(X)$. A necklace diagram is *maximal* if $|\bigcirc| + |\square| = 6n - 2$.

There are 4 maximal E(1) whose necklace diagrams that are depicted on the top line of Figure 6. For $n = 2$ we have:

Proposition 4.9. *There are 10 isomorphism classes of maximal non-directed totally real* E(2) *admitting a real section. Corresponding necklace diagrams are given in Figure 7.* □

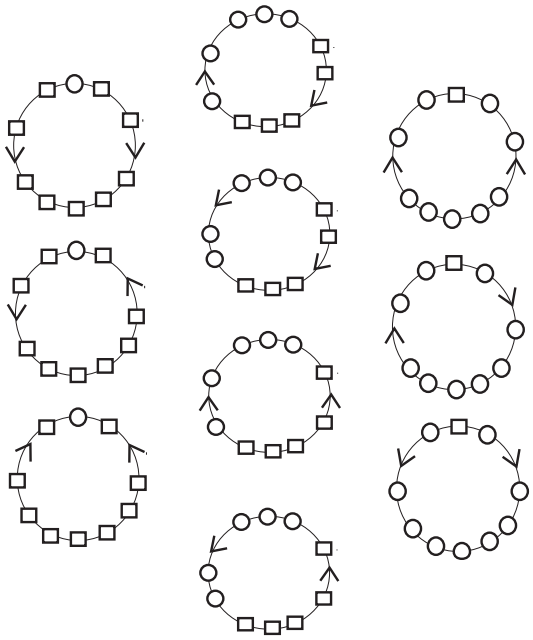

FIG. 7. List of necklace diagrams of maximal totally real E(2) admitting a real section.

5. Applications of necklace diagrams

In this section, we study the algebraic realization of the totally real elliptic Lefschetz fibrations admitting a real section. The crucial observation is that any algebraic elliptic Lefschetz fibration E(n) admitting a real section can be seen as the double branched covering of a Hirzebruch surface of degree $2n$, branched at the exceptional section and a trigonal curve disjoint from the section. In [7], S. Yu. Orevkov introduced a real version of Grothendieck's dessins d'enfants for

the trigonal curves, which are disjoint from the exceptional section, on Hirzebruch surfaces. We apply his result by converting language of real dessin d'enfants to the language of necklace diagrams.

5.1. **Trigonal curves on Hirzebruch surfaces.** The Hirzebruch surface, $H(k)$, of degree k is a complex surface equipped with a projection, $\pi_k : H(k) \to \mathbb{C}\mathrm{P}^1$, which defines a $\mathbb{C}\mathrm{P}^1$-bundle over $\mathbb{C}\mathrm{P}^1$ with a unique exceptional section s such that $s \cdot s = -k$. In particular, $H(0) = \mathbb{C}\mathrm{P}^1 \times \mathbb{C}\mathrm{P}^1$ and $H(1)$ is $\mathbb{C}\mathrm{P}^2$ blown up at one point.

Each Hirzebruch surface $H(k)$ can be obtained from $H(0)$ by a sequence of blow-ups followed by blow-downs at a certain set of points. If these points are chosen to be real, then the resulting Hirzebruch surface has a real structure inherited from the real structure *conj* $\times$ *conj* on $H(0)$. This will be the real structure of our consideration. With respect to this real structure, the real part of $H(k)$ is a torus if k is even; otherwise it is a Klein bottle.

In this note, we only consider nonsingular curves, so by a *trigonal curve* on a Hirzebruch surface $H(k)$ we understand a smooth algebraic curve $C \subset H(k)$ such that the restriction of the bundle projection, $\pi_k : H(k) \to \mathbb{C}\mathrm{P}^1$, to C is of degree 3. A trigonal curve on $H(k)$ is called *real* if it is invariant under the real structure of $H(k)$.

5.2. **Real dessins d'enfants of trigonal curves.** We choose affine (complex) coordinates (x, y) for $H(k)$ such that the equation $x = const$ corresponds to fibers of π_k and $y = \infty$ is the exceptional section s. Then, with respect to such affine coordinates any (algebraic) trigonal curve can be given by a polynomial of the form $y^3 + u(x)y + v(x)$ where u and v are real one variable polynomials such that $deg\, u = 2k$ and $deg\, v = 3k$.

The discriminant of $y^3 + u(x)y + v(x) = 0$ with respect to y is $-4u^3 - 27v^2$. Let $D = 4u^3 + 27v^2$. The fraction $j = \frac{4u^3}{D}$ is the *j-invariant* of a trigonal curve $C \subset H(k)$. The j-invariant defines a real rational function $j : \mathbb{C}\mathrm{P}^1 \to \mathbb{C}\mathrm{P}^1$ whose poles are the roots of D, zeros are the roots of u (taken with multiplicity 3), and the solutions of $j = 1$ are the roots of v (taken with the multiplicity 2).

Let us color $\mathbb{R}\mathrm{P}^1$ as in Figure 8. Then, the inverse image $j^{-1}(\mathbb{R}\mathrm{P}^1)$ turns naturally into an oriented colored graph on $\mathbb{C}\mathrm{P}^1$. Since j is real, the graph is symmetric with respect to the complex conjugation on $\mathbb{C}\mathrm{P}^1$. Around the vertices the graph looks as shown in Figure 9. (Detailed discussion on j-invariant of trigonal curves can be found in [1], [7].)

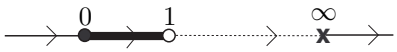

FIG. 8. Coloring of $\mathbb{R}\mathrm{P}^1$.

The following theorem gives the conditions which are sufficient for real algebraic realizability of a graph and the existence of respective polynomials u, v, D.

Theorem 5.1. [7] *Let $\Gamma \subset \mathrm{S}^2$ be an embedded oriented graph where each of its edges is one of the three kinds: ——, ·····, ▬ and some of its vertices are colored by the elements of the set $\{\circ, \bullet, \times\}$, while others remain uncolored. Let Γ satisfy*

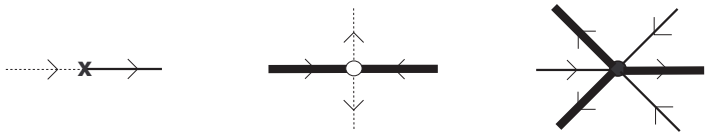

FIG. 9. The graph around the inverse images of zeros of D, v, u, respectively.

the following conditions:

- *the graph* Γ *is symmetric with respect to an equator of* S^2*, which is included into* Γ*;*
- *the valency of each vertex "* $\bullet$ *" is divisible by* 6*, and the incident edges are colored alternatively by incoming* ——*, and outgoing* ▬*;*
- *the valency of each vertex "* $\circ$ *" is divisible by 4, and the incident edges are colored alternatively by incoming* ▬*, and outgoing* .....*;*
- *the valency of each vertex "* $\times$ *" is 2, and the incident edges are colored alternatively by incoming* .....*, and outgoing* ——*;*
- *the valency of each non-colored vertex is even, and the incident edges are of the same color;*
- *each connected component of* $\mathrm{S}^2 \setminus \Gamma$ *is homeomorphic to an open disk whose boundary is colored as a covering of* $\mathbb{R}\mathrm{P}^1$ *(colored and oriented as in Figure 8) and the orientations of the boundaries of neighboring disks are opposite.*
  Then, there exists a real rational function $j = \frac{4u^3}{D}$ *whose graph is* Γ*. (And thus, there exist a non-singular real algebraic trigonal curve associated to the* j*-invariant.)*

Definition 5.2. A graph on S^2 satisfying the six conditions of the above theorem is called a *real dessin d'enfant.*

Remark 5.3. Let us accentuate the fact that there is no relation between the decorations "$\times$", "$\circ$" of the critical values that we use to introduce the necklace diagrams and the coloring of the vertices of the real dessin d'enfants considered in this section.

5.3. **Relation to the real scheme.** The real scheme of a trigonal curve imposes strong restrictions on the arrangement of the real roots of u, v and D. For example, the zeros of D correspond to the points where the trigonal curve is tangent to the fibers of $\pi_k : H(k) \to \mathbb{C}\mathrm{P}^1$. A typical correspondence for certain model pieces of the curve is shown in Figure 10. Because the graph is symmetric with respect to the equator, we consider the part of the graph lying on one of the semi-disks.

As we mention in the previous section, necklace diagrams encode the topology of the real part (except orientability) of $\mathrm{E}(n)$ which admit a real section. Indeed, the real part of totally real $\mathrm{E}(n)$, admitting a real section, consists of spherical

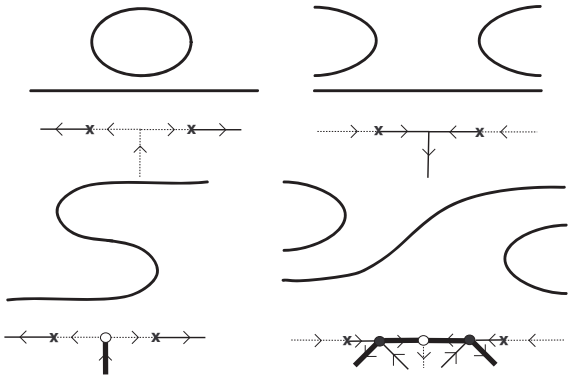

FIG. 10. Segments of the curve corresponding to fragments of the minimal graphs.

components (the number of which is $|\bigcirc|$) and a higher genus component which is an orientable surface of genus $|\square| + 1$ if n is even; a non-orientable surface with $2(|\square| + 1)$ cross-caps, otherwise.

Definition 5.4. A segment of a necklace chain is called *essential* if it is one of the segments shown in Figure 11.

FIG. 11. Essential segments.

5.4. **Applications.**

Proposition 5.5. *If a real elliptic Lefschetz fibration,* $\mathrm{E}(n)$*, admitting a real section is algebraic then the corresponding necklace diagram has the following properties:*

- *there are not more than* $2n$ *essential segments,*
- *the sum of the number of essential segments and the number of arrow-type stones cannot be greater than* $6n$*.*

Proof: For a trigonal curve on $H(2n)$ defined by $y^3+u(x)y+v(x)$, $deg\, u = 2\cdot 2n$ and $deg\, v = 3 \cdot 2n$. Thus, the real dessin d'enfant can have at most $4n$ vertices colored by "$\bullet$" and at most $6n$ vertices colored by "$\circ$". The result follows from the observation that each essential interval corresponds to a graph fragment which contains at least two "$\bullet$" type vertices and at least one "$\circ$" type vertex, while each arrow-type stone corresponds to a fragment having at least one "$\circ$" type vertex, see [1]. □

By listing the necklace diagrams violating the conditions of Proposition 5.5, we get:

Corollary 5.6. *The totally real elliptic Lefschetz fibrations corresponding to the necklace diagrams depicted in Figure 12 are not realized algebraically.*

□

FIG. 12. The last diagram violates the second condition, while all the others violate the first one.

Lemma 5.7. *If a totally real elliptic Lefschetz fibration admitting a real section is algebraic then the totally real elliptic Lefschetz fibration whose necklace diagram is dual to the necklace diagram of the former is also algebraic.*

Proof: The crucial observation is that although the real parts of fibrations associated with dual necklace diagrams are topologically different, trigonal curves appearing as the branching set of coverings $\mathrm{E}(n) \to H(2n)$ are the same. Duality of necklace diagrams corresponds, indeed, to the two different liftings of the real structure of $H(2n)$ to $\mathrm{E}(n)$, see Figure 13. Thus, the result follows. □

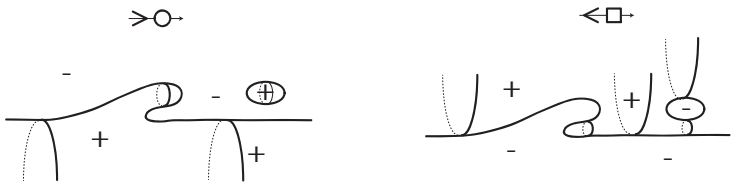

FIG. 13. For each trigonal curve on $H(2n)$, there are two real structures of $\mathrm{E}(n)$.

Theorem 5.8. *All totally real* $\mathrm{E}(1)$ *admitting a real section are algebraic except those fibrations whose necklace diagram is one of the diagrams listed in Figure 12.*

Proof: By Theorem 5.1 it is enough to construct real dessins d'enfants corresponding to necklace diagrams which are not prohibited by Proposition 5.5. Following Lemma 5.7, we only need to consider necklace diagrams with $|\bigcirc| \geq |\square|$. Figures 14-15 show the required real dessins d'enfants. (In the figures, the real part is depicted around necklace diagrams. The dotted inner circle stands for the lift of the exceptional section. Because of the symmetry, we only draw a half of the graph.) □

6. Necklace calculus and further applications

In this section, we consider certain operations on the set of necklace diagrams. These operations allow us to construct new necklace diagrams from the given ones.

6.1. **Necklace sums.** A *necklace sum* is basically the connected sum of the underlying oriented circle and it refers to the fiber sum of the corresponding real Lefschetz fibrations. We consider two types of necklace sums which we call *mild sum* and *harsh sum*. To perform a mild sum, we cut each necklace diagram at a point on the chain then reglue the diagrams crosswise respecting the orientation. The harsh sum, on the other hand, is obtained by cutting necklace diagrams at

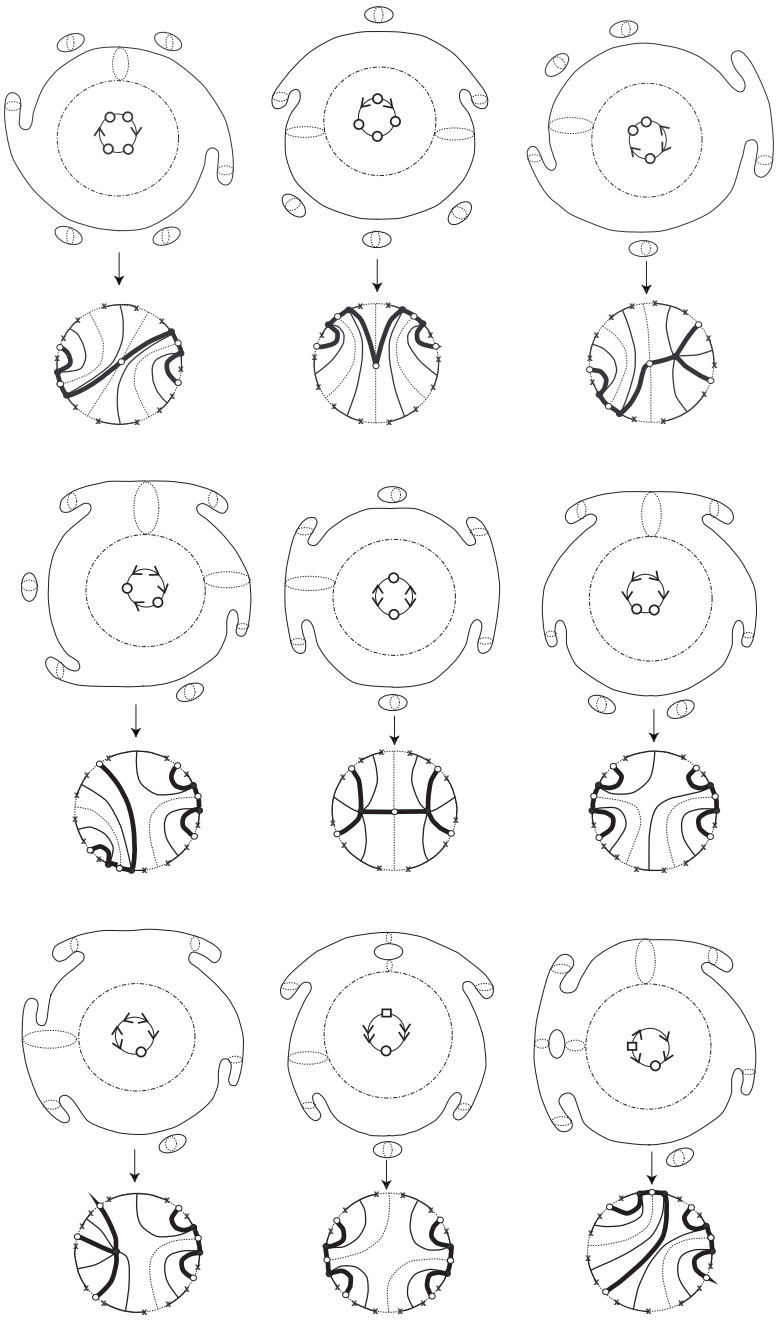

FIG. 14. Real dessin d'enfants.

a stone and regluing them according to the table shown in Figure 16. It follows from their definition that both the mild sum and the harsh sum do not change the

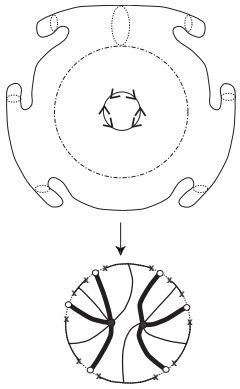

FIG. 15. Real dessin d'enfants.

monodromy of the diagram. Evidently, the Euler characteristic of the real part $X_{\mathbb{R}}$ is additive with respect to the mild sum; however, it is not always additive with respect to the harsh sum.

Let us note also that we can also consider necklace sum of non-oriented necklace diagrams by fixing auxiliary orientations on diagrams.

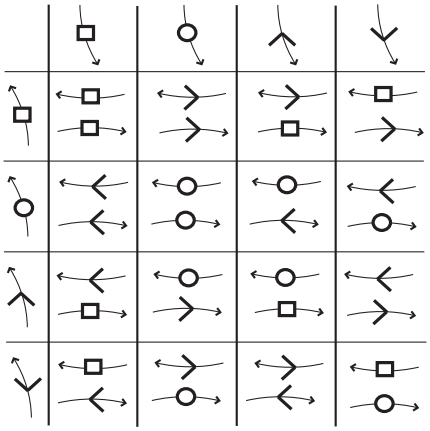

FIG. 16. Table of the harsh sum

Examples of mild and harsh sums are given in Figure 17.

Remark 6.1. There are two types of necklace chain segments (essential, non-essential). It is not hard to see that the mild sum preserves algebraic realizability if the points where the sum is taken are chosen on the same type of chain segments and if the segments after the sum remain of the same type; or if they are chosen on different types of chain segments. In other words, algebraic realizability is preserved if we make a mild sum at two essential (respectively, non-essential) intervals, in a way that after gluing we obtain again two essential (respectively, non-essential) intervals; or if we make sum at an essential and a non-essential intervals. As for the harsh sum, we note that it preserves algebraic realizability if the number of neither ○-type nor □-type stone decreases after the sum.

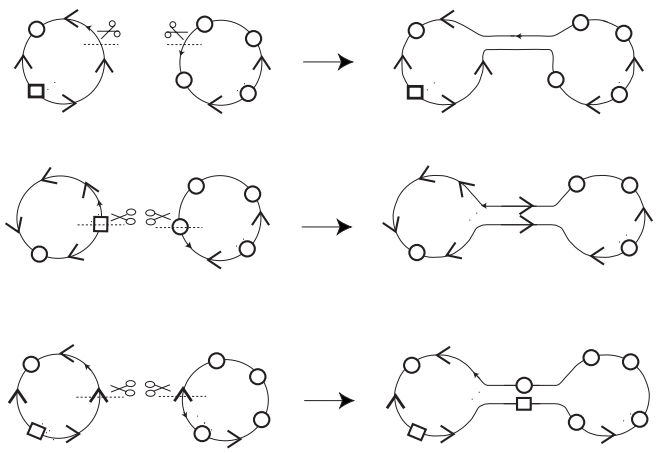

FIG. 17. Examples of the mild and the harsh sums.

Proposition 6.2. *For each n, maximal necklace diagrams exist and each totally real elliptic* $\mathrm{E}(n)$ *represented by a maximal necklace diagram is algebraic.*

Proof: It is easy to see that the harsh sum of two maximal necklace diagrams where the sum is performed at arrow-type stones of the opposite directions is maximal. Moreover, by the remark above the harsh sum performed at two arrow-type stones of opposite directions preserves algebraic realizability. Note also that as Theorem 5.8 asserted all maximal necklace diagrams of 6 stones are algebraic.

To finish the proof, we show that all maximal necklace diagrams of n stones are obtained as harsh sums of maximal necklace diagrams of 6 stones. We will prove the claim by induction on n. The first step is to check the claim for $n = 2$. As we have the explicit list of maximal diagrams of 12 stones, we see immediately that any maximal necklace diagram of 12 stones can be obtained as the harsh sum of maximal necklace diagrams of 6 stones. Now, let us assume that for $n = k$ the claim is true. To prove the claim for $n = k+1$, note that the monodromies of $\bigcirc$-type stones and $\square$-type stones do not have any cancelation. The fact that the monodromy of the necklace diagram is the identity and that there is no cancellation between the monodromy of $\bigcirc$-type stones and the monodromy of $\square$-type stones impose certain conditions on the possible arrangements of stones around an arrow-type stone on a maximal necklace diagram. By checking the possibilities of the neighborhood of an arrow-type stone, we see that required cancelations appear only in the cases where the arrangements come from the maximal necklace diagrams of 6 stones, so the claim follows from the inductive step. □

6.2. **Flip-flops and metamorphoses.** Let $\mathcal{N}_k$ denote the set of (oriented) necklace diagrams with k stones and with the identity monodromy, and let $\mathcal{N}_k^{(i,j)}$ be the subset consisting of diagrams with $(|\bigcirc|, |\square|) = (i, j)$. We define two kinds of operations on $\mathcal{N}_k$: *flip-flop* and *metamorphosis*. The flip-flop preserves $(|\bigcirc|, |\square|)$ and it coincides with canceling and creating handles on the real part $\mathrm{E}(n)_{\mathbb{R}}$. On the other hand, the metamorphosis decreases $|\bigcirc|$ or $|\square|$ by one and it appertains to a nodal deformation of $\mathrm{E}(n)_{\mathbb{R}}$.

We define *flip-flop* as the operation which swaps the segments shown below. Because the segments have the same monodromy, the total monodromy does not change. Examples of flip-flop are shown in Figure 18.

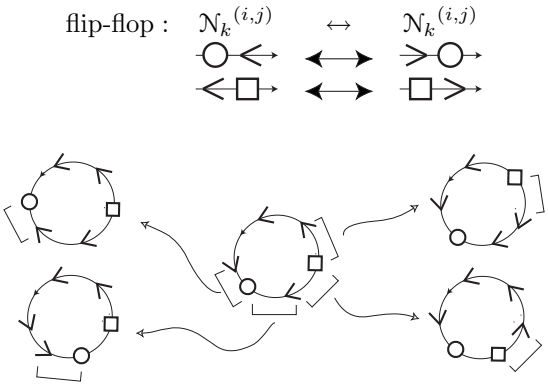

FIG. 18. Examples of flip-flops.

As $|\bigcirc|$ and $|\square|$ remain unchanged after a flip-flop, the Euler characteristic and the total Betti number of the corresponding $\mathrm{E}(n)_{\mathbb{R}}$ do not change. Thus, topological type of $\mathrm{E}(n)_{\mathbb{R}}$ is not affected by the flip-flop. In Figure 19, we interpret the effect of a flip-flop on $\mathrm{E}(n)_{\mathbb{R}}$.

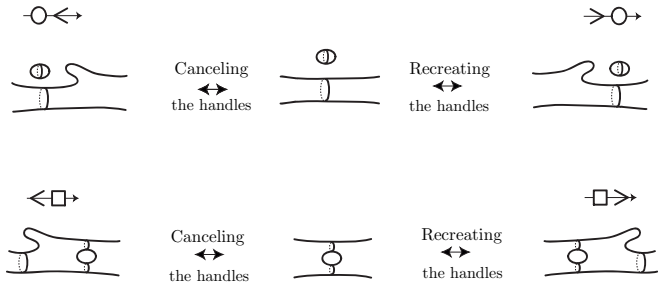

FIG. 19. The effect of flip-flop on the real part.

We consider two types of *metamorphoses*, m_1, m_2, of necklace diagrams. They modify the above segments as follows. Examples of metamorphoses are depicted in Figure 20.

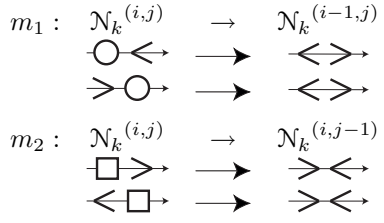

Since $|\bigcirc|$ or $|\square|$ are modified by metamorphoses, the topological type of the corresponding $\mathrm{E}(n)_{\mathbb{R}}$ changes. Recall that for fibrations which admit a real section

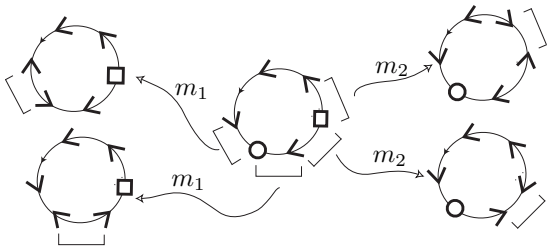

FIG. 20. Examples of metamorphoses.

each ○-type stone corresponds to a spherical component while each □-type stone drives a handle. Indeed, a sphere component or a genus disappears after a metamorphosis (or appears after a inverse metamorphosis). In Figure 21, we depict the effects of metamorphoses on $\mathrm{E}(n)_{\mathbb{R}}$.

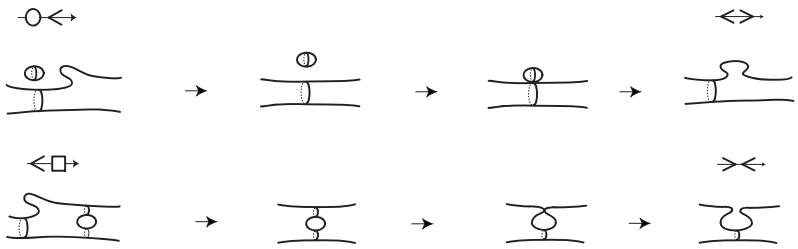

FIG. 21. The effect of metamorphoses, m_1, m_2, to the real part.

6.3. **Applications.** Below, in Figure 22 and Figure 23, we present two graphs (for E(1) and E(2), respectively) whose vertices correspond to necklace diagrams with fixed $(|\bigcirc|, |\square|)$, and edges to necklace metamorphoses m_1, m_2. As we mention before the real part of totally real $\mathrm{E}(n)$, admitting a real section, consists of spherical components (the number of which is $|\bigcirc|$) and a higher genus component which is an orientable surface of genus $|\square| + 1$ if n is even; a non-orientable surface with $2(|\square| + 1)$ cross-caps, otherwise. Each pair $(|\bigcirc|, |\square|)$ and the parity of n, thus, defines the topological type of $\mathrm{E}(n)_{\mathbb{R}}$.

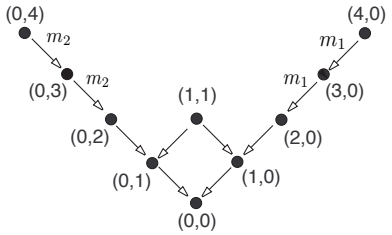

FIG. 22. Metamorphosis graph of $\mathrm{E}(1)_{\mathbb{R}}$.

Examining the list of necklace diagrams of 6 stones we obtain the following:

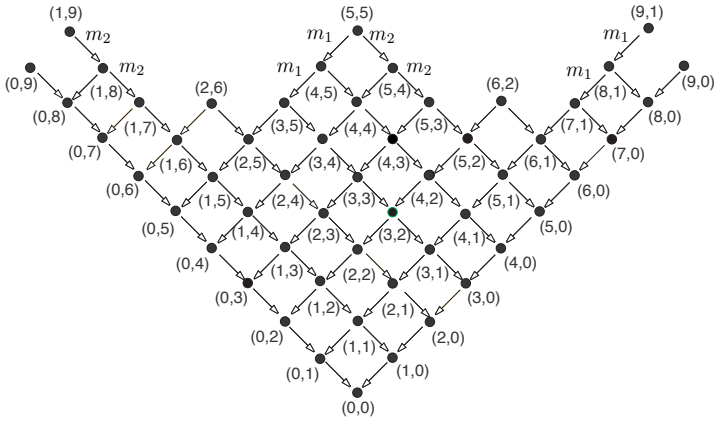

FIG. 23. Metamorphosis graph of $\mathrm{E}(2)_{\mathbb{R}}$.

Proposition 6.3. *All 6-stone necklace diagrams listed in Figure 6 can be obtained from the maximal ones by a sequences of metamorphoses, inverse metamorphoses or flip-flops. Moreover, the list of necklace diagrams which are obtained from maximal diagrams only by a sequence of metamorphoses and eventually an inverse metamorphosis, coincide with the list of diagrams of algebraic fibrations.* □

Proposition 6.4. *There exist 12-stone necklace diagrams (with the identity monodromy) that cannot be obtained from the maximal necklace diagrams by necklace operations.*

Proof: Examples, shown in Figure 24, are found by investigating the list of 12-stone necklace diagrams basically with $(|\bigcirc|, |\square|) = (9,1), (9,0), (8,1), (8,0)$. (By duality it is enough to consider the case of $|\bigcirc| \geq |\square|$.) The fibrations associated with the diagrams shown in Figure 24 are algebraic. □

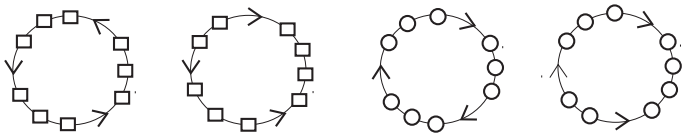

FIG. 24. Diagrams that cannot be obtained by necklace operations.

As a corollary of the above proposition we claim that all totally real algebraic E(1) admitting a real section can be obtained from the maximal ones by a sequences of nodal deformations, while there are totally real algebraic E(2) which cannot be obtained in this way.

Proposition 6.5. *There exist 12-stone necklace diagrams (with the identity monodromy) which are not a necklace sum of two 6-stone necklace diagrams listed in Figure 6.*

Proof: In Figure 25, we construct a non-decompasable example applying a mild sum followed by a flip-flop. Let us also note that such examples can be produced the same way for any $n > 1$.

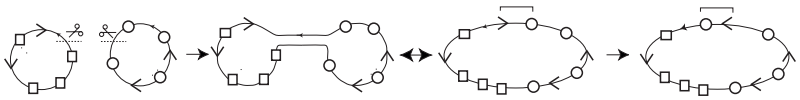

FIG. 25. An example of construction of a non-decomposable necklace diagram.

Using the list of necklace diagrams of 6 stones (see Figure 6) and by analyzing possible divisions of the pair $(|\bigcirc|, |\square|)$, we see that the 12-stone necklace diagram shown in Figure 25 cannot be divided into two 6-stone necklace diagrams with the identity monodromy. □

Corollary 6.6. *There exist totally real* E(2) *which cannot be written as a fiber sum of two totally real* E(1). □

7. Totally real elliptic Lefschetz fibrations without a real section and refined necklace diagrams

In this section, we explore the case of totally real elliptic Lefschetz fibrations $\pi : X \to \mathrm{S}^2$ which do not admit a real section and introduce *refined necklace diagrams* associated with them.

A refinement of a necklace diagram is obtained by replacing each ○-type stone with one of the following refined stones, ○, ⊘, ◌, ◌. If the refined necklace diagram is identical to the underlying necklace diagram then the corresponding real Lefschetz fibration admits a real section. Examples of refinements of a necklace diagram are shown in Figure 26.

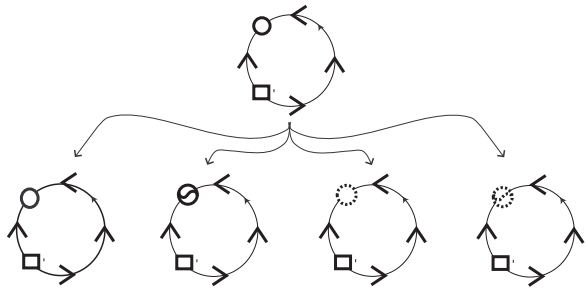

FIG. 26. Refinement of a necklace diagram.

From Remark 3.2, it is clear that if a real structure on a fiber of π has no real component, then the nearby critical values can only be of type "∘". In other words, existence or lack of a real section influences only ○-type necklace stones.

Both of the refined stones of type ○, ⊘ correspond to the case where the real structure on the real fibers over the interval between the two critical values has 2

real components. Already the real part $X_{\mathbb{R}}$ of X distinguishes the cases of ○ and ⊘, see Figure 27. (In Figures 27 and 28 below, the dotted part depicts the traces of the curves on which the inherited real structure acts as the antipodal map.) As notation suggested ○ has to do with the case where there is a real section, and hence, only ○-type refined stones refer to a spherical component of $X_{\mathbb{R}}$.

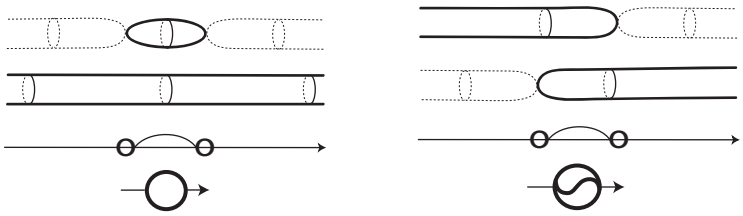

FIG. 27. Real part and associated refined stones.

Recall that if the condition that the fibration admits a real section is discarded, then the fibers of $\pi_{\mathbb{R}}$ may also be empty (which happens when the real structure on the real fibers of π has no real component). We introduce the refined stones ◌ and ⊘ which correspond to the case where the real structure on the real fibers of π has no real component. As depicted in Figure 28, the real part of $X_{\mathbb{R}}$ does not distinguish the two situations associated with ◌, ⊘. The difference between ◌ and ⊘ (as well as between ○ and ⊘) can indeed be conceived by comparing the equivariant isotopy classes of the two vanishing cycles corresponding to the two critical values of the necklace stone. In the case of ◌ (respectively, ○) the equivariant isotopy classes of the two vanishing cycles are the same, while in the case of ⊘ (respectively, ⊘) the two vanishing cycles are of different equivariant classes. (A more detailed discussion can be found in [6, Section 8].)

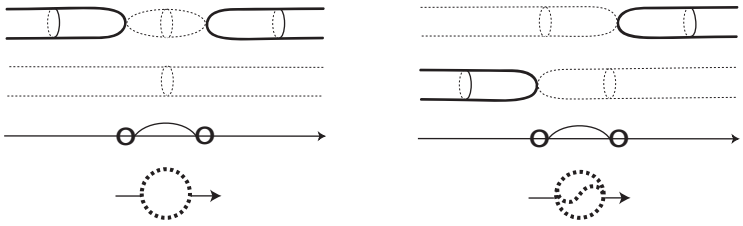

FIG. 28. Real part and associated refined stones.

As mentioned in Remark 3.7, there is no difference between real structures with 2 real components and real structures with no component on the homological level. As a consequence, the calculation of the monodromy is not affected by the refinement. Thus, we have the following theorem.

Theorem 7.1. *There is a one-to-one correspondence between the set of oriented refined* $6n$*-stone necklace diagrams whose monodromy is the identity and the set of isomorphism classes of directed totally real* $\mathrm{E}(n)$*,* $n \in \mathbb{N}$*.*

Proof: The proof is analogous to the proof of Theorem 4.1. It is obvious from its construction that the refinements of necklace diagram is exactly the decoration

of the real Lefschetz chains, see [6, Figure 10]. Thus, we relate refined necklace diagrams with the *decorated real Lefschetz fibrations*, complete invariants of totally real elliptic Lefschetz fibrations, presented in [6, Section 8]. The result, thus, follows from Theorem 8.1 and Proposition 8.2 of [6]. □

Corollary 7.2. *There is a one-to-one correspondence between the set of symmetry classes of non-oriented refined* $6n$*-stone necklace diagrams whose monodromy is the identity and the set of isomorphism classes of totally real* $\mathrm{E}(n)$*,* $n \in \mathbb{N}$*.* □

Below, for each fixed $(|\bigcirc|, |\square|)$, we give the number of possible refinements of 6-stone necklace diagrams.

- $(|\bigcirc|, |\square|) = (1, 1)$ there are 12 refined necklace diagrams;
- $(|\bigcirc|, |\square|) = (1, 0)$ there are 8 refined necklace diagrams;
- $(|\bigcirc|, |\square|) = (2, 0)$ there are 46 refined necklace diagrams;
- $(|\bigcirc|, |\square|) = (3, 0)$ there are 84 refined necklace diagrams;
- $(|\bigcirc|, |\square|) = (4, 0)$ there are 251 refined necklace diagrams.

References

[1] Degtrayev, A.; Itenberg I.; Kharlamov V. *On Deformation types of real elliptic surfaces.* American Journal of Mathematics, Volume 130, Number 6, 2008, 1561-1627.

[2] Gompf, R.E., A.I. Stipsicz *4-manifols and Kirby calculus.* Amer. Math. Soc. Grad. Stud. in Math. 20 Rhode Island, (1999).

[3] Kulikov, S.; Kharlamov, V. *On real structures on rigid surfaces.* (Russian) Izv. Ross. Akad. Nauk Ser. Mat. 66 (2002), no. 1, 133–152; translation in Izv. Math. 66 (2002), no. 1, 133150.

[4] Moishezon, B. *Complex surfaces and connected sums of complex projective planes.* Lecture notes in Math. 603 Springer Verlag(1977).

[5] Salepci, N. *Real classes in the mapping class group of* T^2, Topology and its Applications, Volume 157, Issue 16, 2010, 2480-2590.

[6] Salepci, N. *Invariants of totally real Lefschetz fibrations*, to appear in Pacific J. of Math.

[7] Orevkov, S.Yu. *Riemann existence theorem and construction of real algebraic curves.* Ann. Fac. Sci. Toulouse Math. (6)12, 2003, no. 4, 517-531.

Institut Camille Jordan, Université Lyon I, 43, Boulevard du 11 Novembre 1918 69622 Villeurbanne Cedex, France

E-mail address: salepci@math.univ-lyon1.fr